Asian Summer Monsoon

Fig. 1: JJAS Precipitation climatology/JJAS Precipitation standard deviation (20S-50N, 40E-160E)

Fig. 2: JJAS SST climatology/uv850 climatology (20S-50N, 40E-160E)

Fig. 3: Scatterplot of the pattern correlation pr clim vs. pattern correlation uv850

Fig. 4: Annual Cycle Monsoon domain and intensity (20S-50N, 40E-160E) (obs, mean model, best model, worst model)

Fig. 5: Pattern correlation MPI vs. threat score

Fig. 6: Monsoon Onset using pentad rainfall

Fig. 7: Monsoon-ENSO relationship: Lead-lag AIR vs. NINO3.4 SST

Fig. 8: Monsoon-ENSO relationship: NINO3.4 correlations with local precip anomalies

Fig. 9: Intraseasonal Variability: 20-100 day variance

Fig. 10: Intraseasonal Variability: Northward propagation

Fig. 11: Intraseasonal Variability: Tilted rainband

Table: Space-time correlation of simulated vs. observed life-cycle patterns of BSISV

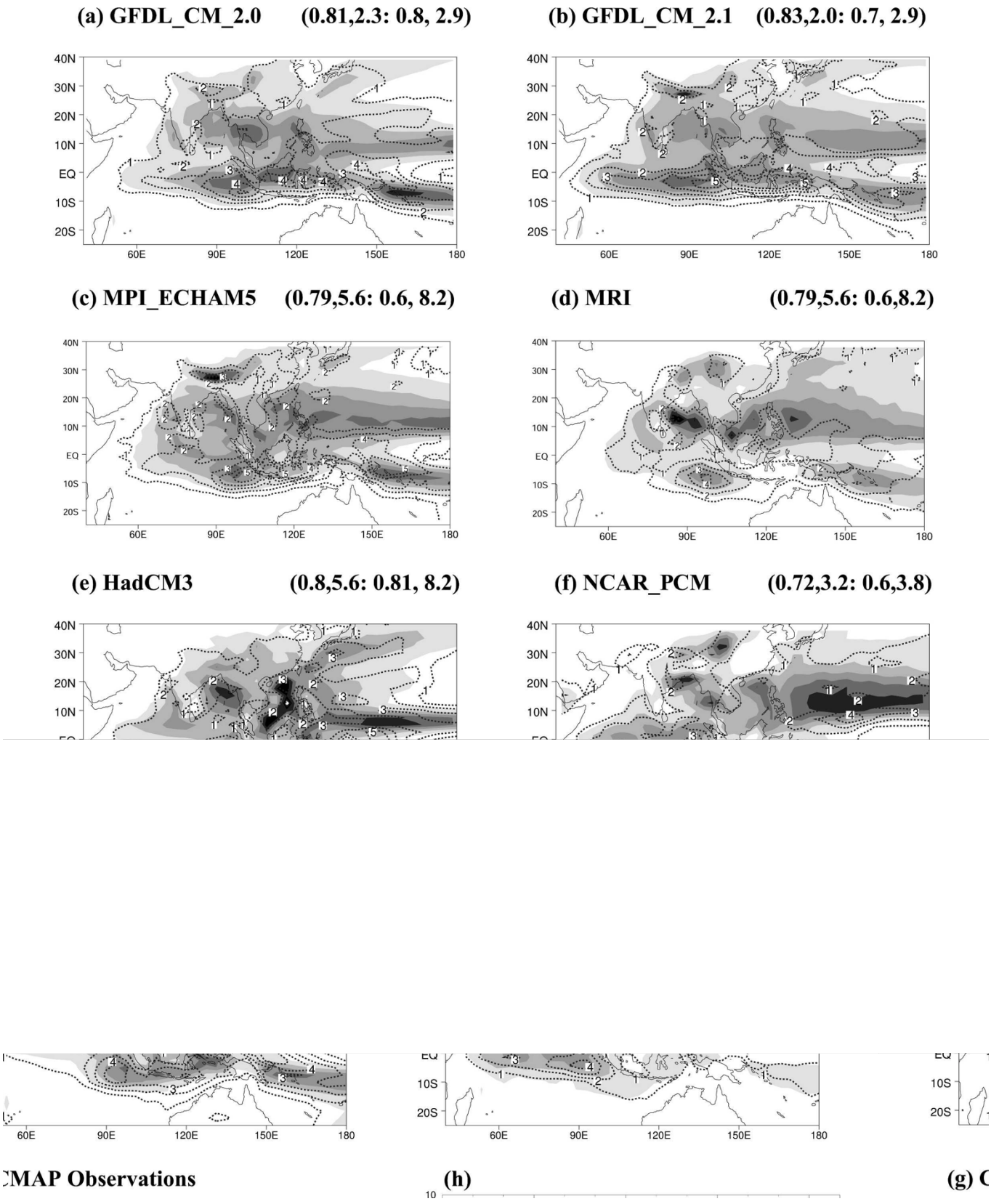

Figure 1: (a) – (g) JJAS precipitation rate climatology (mm day-1, shading), and standard deviation (contours). After Annamalai et al. (2007). (h) Annual cycle of rainfall over 60E-100E, 10N-25N).

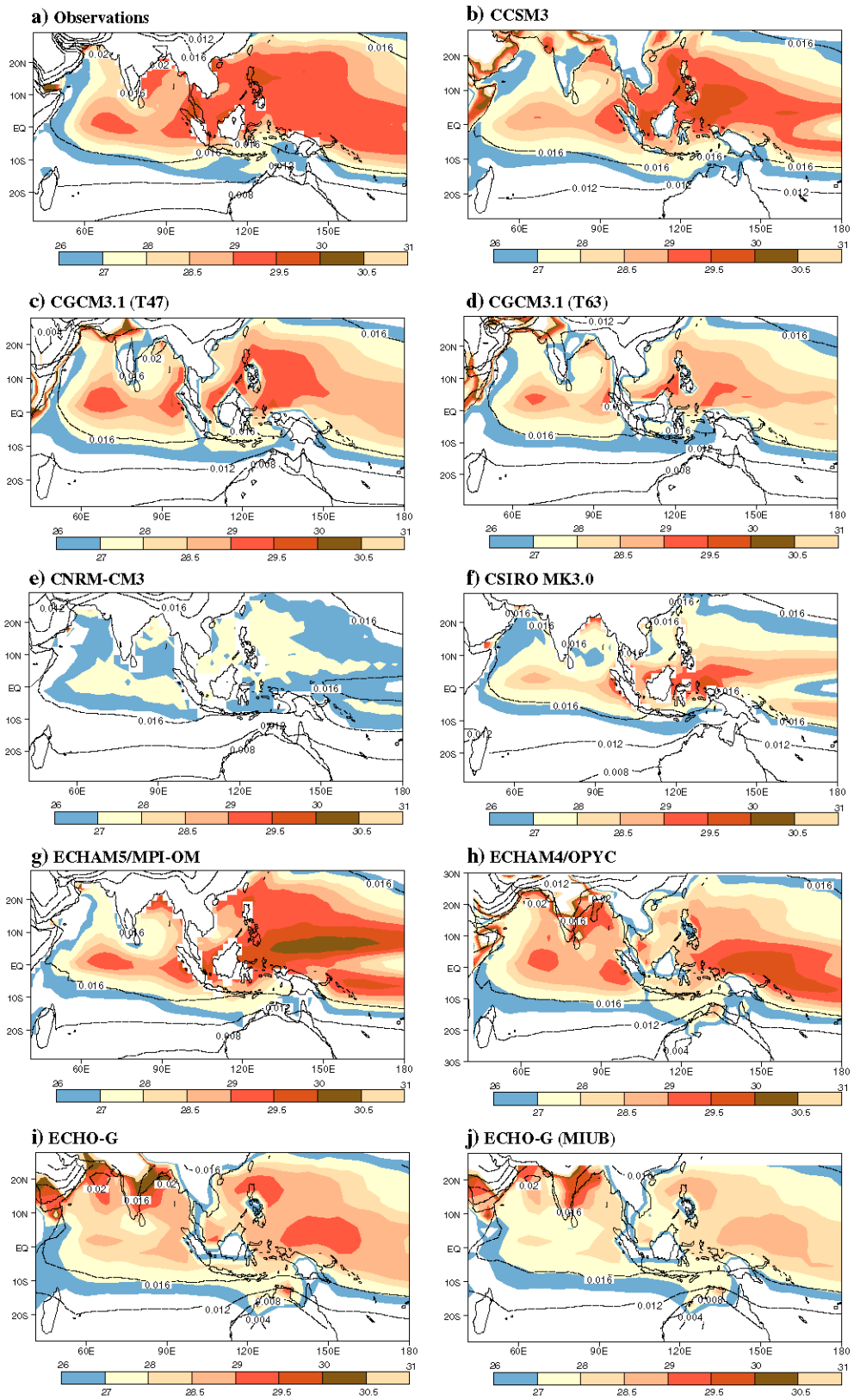

Figure 2: JJAS SST climatology (^{o}C, shading), and 850hPa wind vectors. After Sperber and Annamali (2008).

Figure 3: Scatterplot of the pattern correlation with observations of simulated JJAS pr climatology vs. the pattern correlation with observations of simulated JJAS uv850.

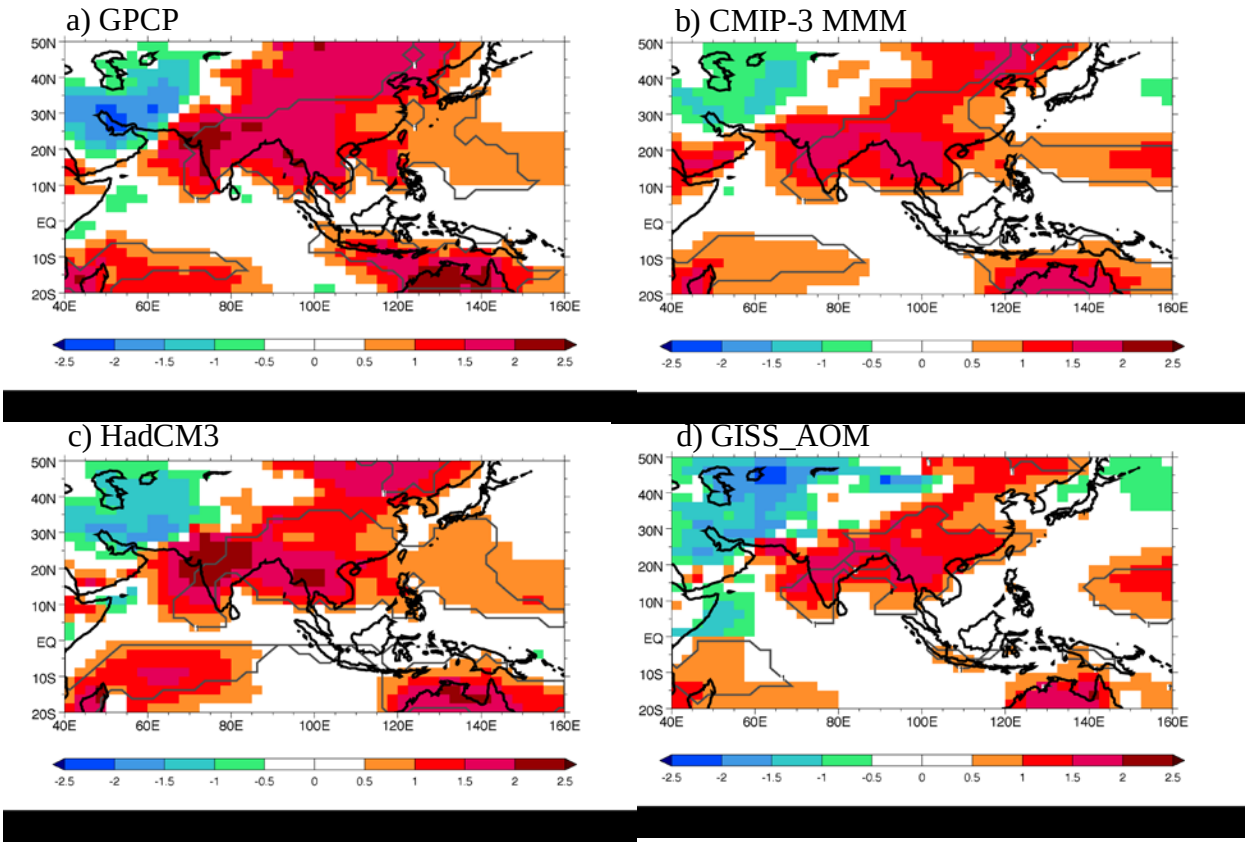

Figure 4: Monsoon precipitation intensity (shading) and monsoon precipitation domain (isoline) are plotted for (a) GPCP, (b) the CMIP-3 multi-model mean, the HadCM3 model, and (d) the GISS-AOM model. See Wang and Ding (2008), Wang et al. (2010), and Kim et al. (2011) for more details of the calculations.

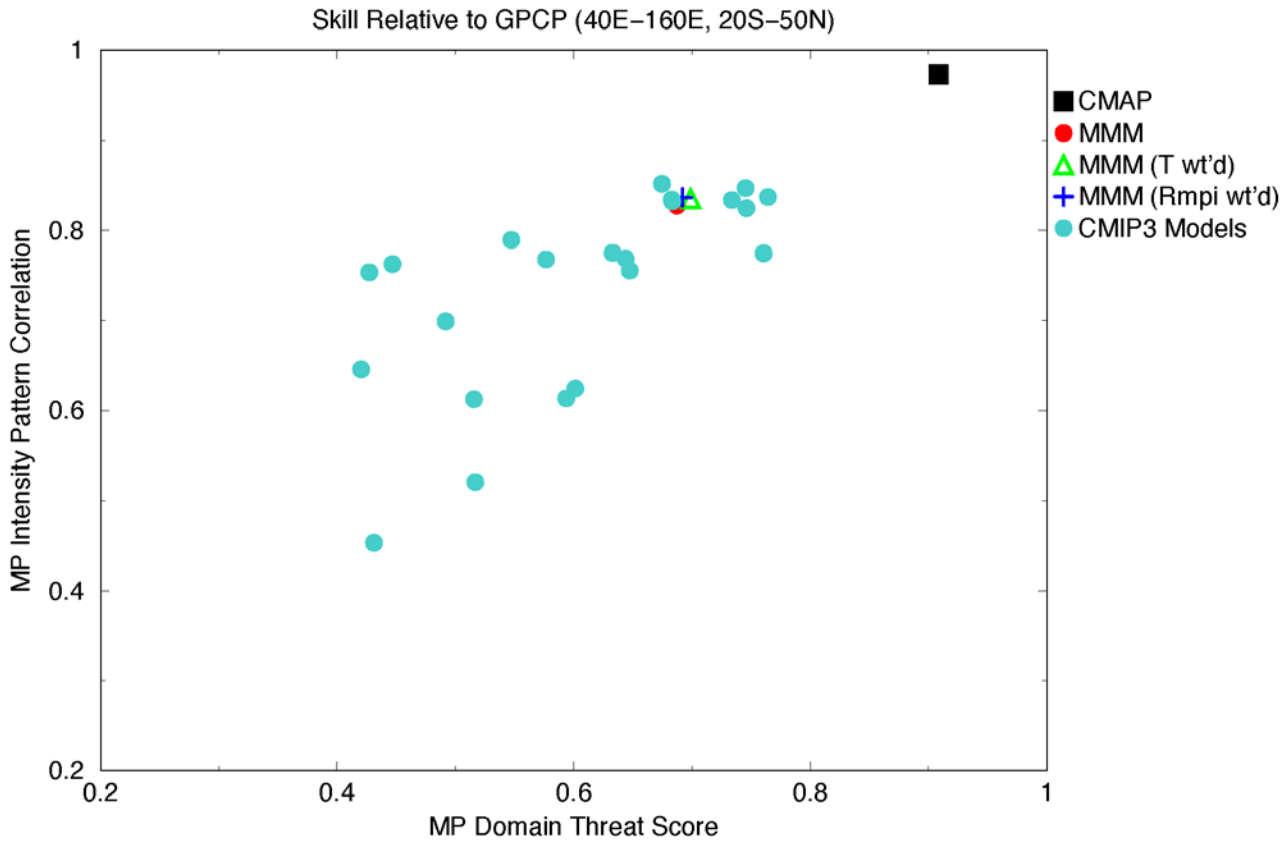

Figure 5: Monsoon Precipitation Intensity pattern correlation plotted as a function of the Monsoon Precipitation Domain Threat Score over the region 40°E-160°E, 20°S-50°N. The skill is plotted relative to GPCP rainfall from CMAP, the CMIP3 multi-model mean (MMM), the MMM weighted by the threat score, the MMM weighted by the Monsoon Precipitation Intensity pattern correlations, and form each of the CMIP3 models.

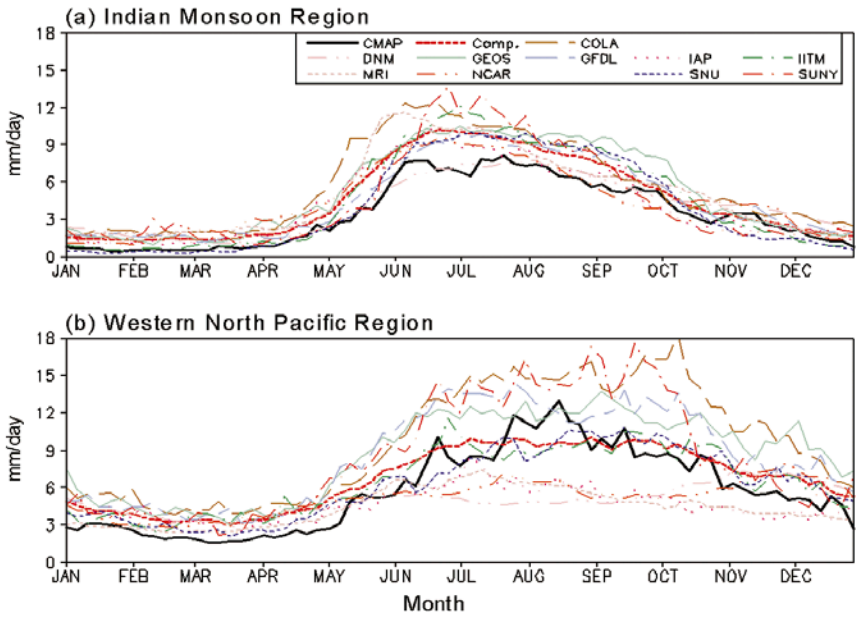

Figure 6: Climatological pentad mean precipitation anomalies (mm/day) from CMAP, the CMIP3 models and the CMIP3 multi-model mean for 1979-2007. The IMI region is 60^{o}E-105^{o}E, 7.5^{o}N-27.5^{o}N; the WNP region is 105^{o}E, 150^{o}E, 7.5^{o}N-25^{o}N). We need to discuss region domain in light of Andy's comment regarding the Himalayas. After Wang et al. (2004).

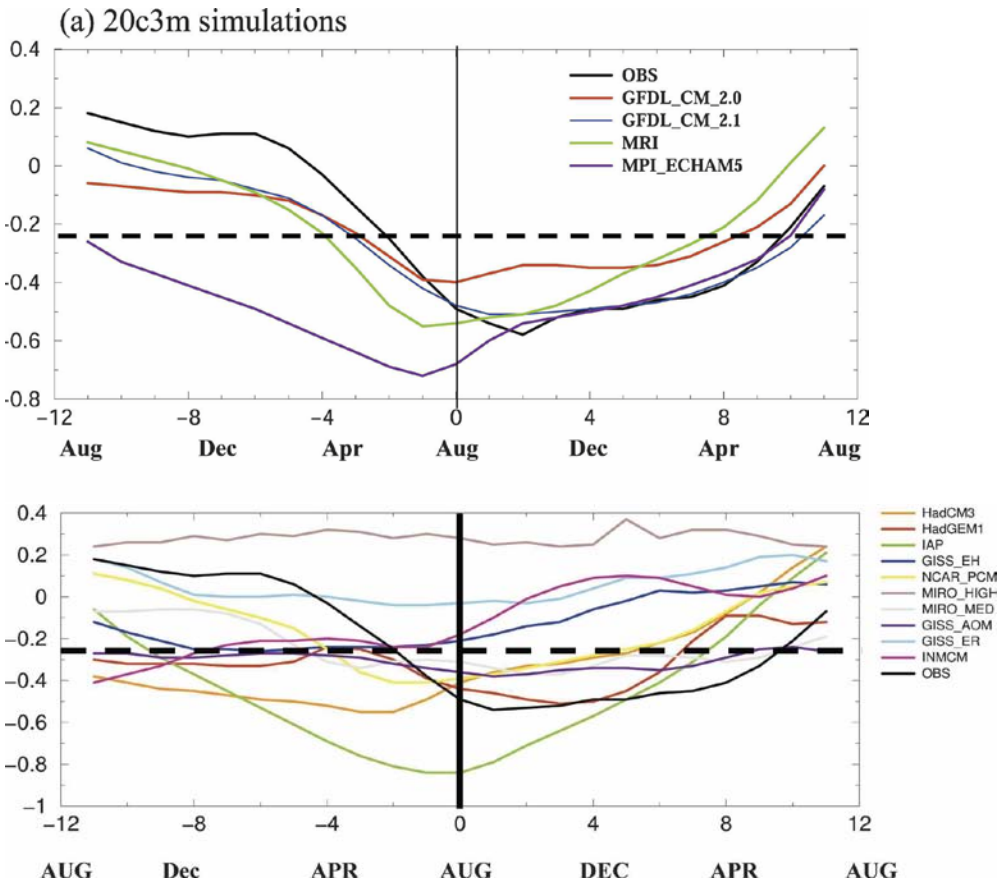

Figure 7: Lead-lag correlation between monthly anomalies of AIR and NINO3.4 SST. (a) models with realistic monsoon precipitation climatology and ENSO variability. (b) Models with either a poor monsoon precipitation climatology and/or unrealistic ENSO variability. The AIR region is 65^{o}E-95^{o}E, 7^{o}N-30^{o}N. After Annamalai et al. (2007).

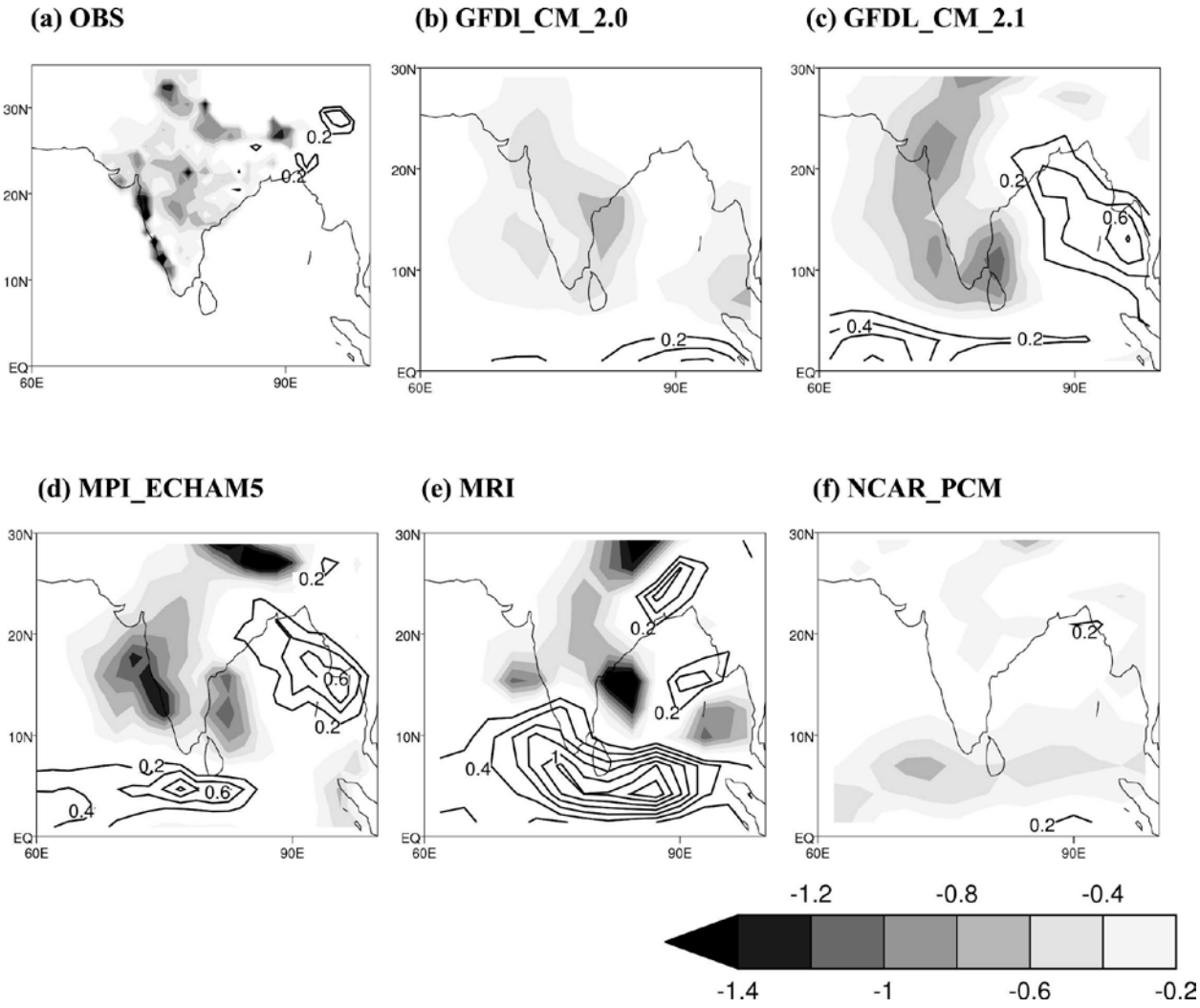

Figure 8: JJAS precipitation anomalies via regression with JJAS NINO3.4 SST anomalies. After Annamalai et al. (2007).

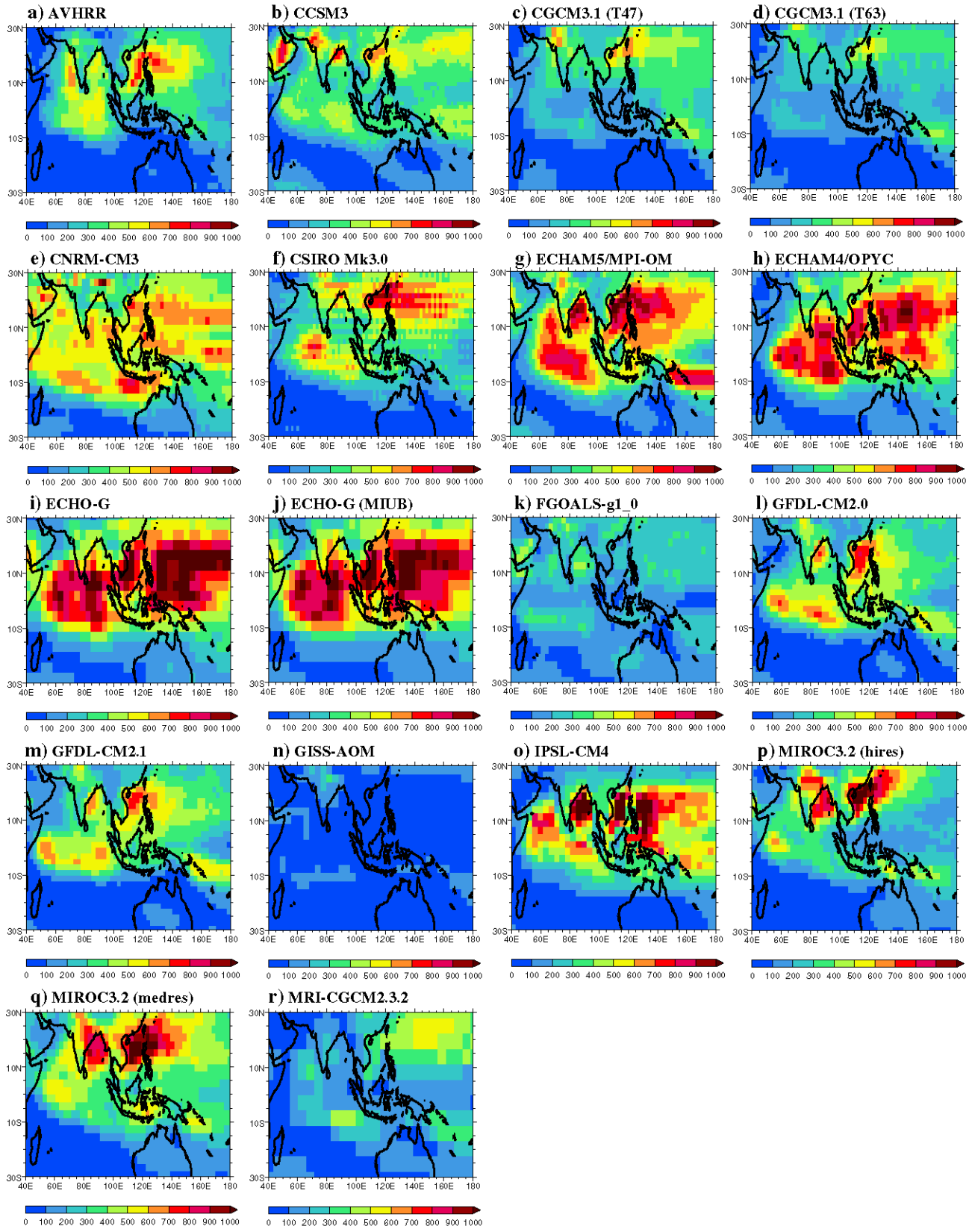

Figure 9: JJAS 20-100 day filtered variance of OLR. After Sperber and Annamalai (2008).

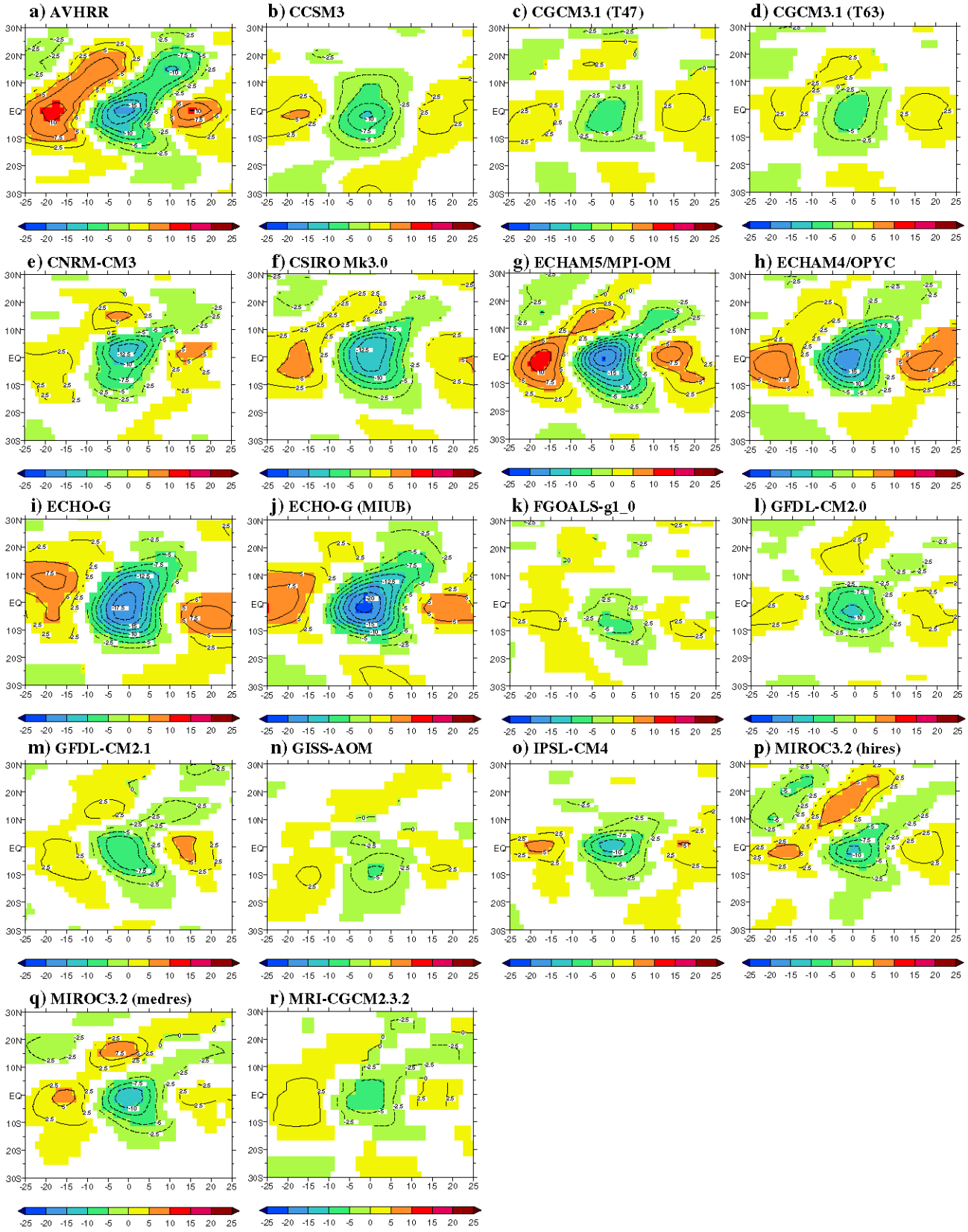

Figure 10: Latitude-time lag regression plots of 71.25oE-83.75E averaged 20-100 day OLR anomalies (Wm-2) with PC-4. lag regressions have been scaled by 1 standard deviation of PC-4. After Sperber and Annamalai (2008).

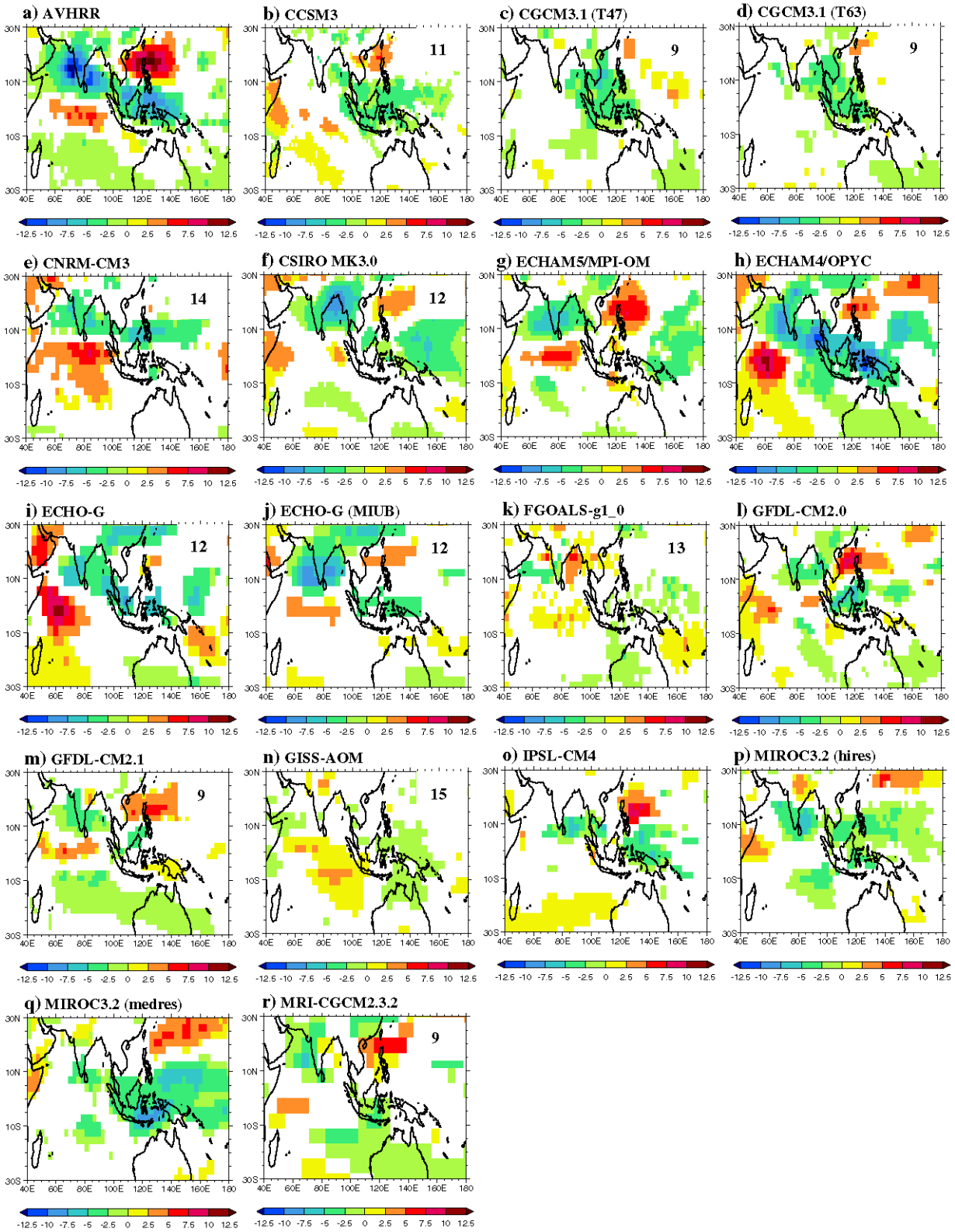

Figure 11: Titled rainband 20-100 day filtered OLR. After Sperber and Annamalai (2008).

Table 3 Space–time correlation for PC-4 regressed patterns of BSISV from models and observations relative to the CsEOF's for day 10 (column 2), and for the full space-time pattern correlation for day −15 through day 20 in increments of 5 days over the region 40°E–180°W, 10°S–30°N (column 3)

Model designation	Pattern correlation day 10	Pattern correlation days −15 to 20
AVHRR	0.90	0.91
CCSM3.0	0.42	0.60
CGCM3.1 (T47)	0.33	0.62
CGCM3.1 (T63)	0.30	0.60
CNRM-CM3	0.28	0.61
CSIRO Mk3.0	0.32	0.59
ECHAM5/MPI-OM	0.66	0.72
ECHAM4/OPYC	0.54	0.72
ECHO-G	0.36	0.66
ECHO-G (MIUB)	0.61	0.71
FGOALS-g1.0	0.26	0.46
GFDL-CM2.0	0.56	0.69
GFDL-CM2.1	0.64	0.72
GISS-AOM	0.28	0.42
IPSL-CM4	0.65	0.66
MIROC3.2 (hires)	0.28	0.55
MIROC3.2 (medres)	0.34	0.58
MRI-CGCM2.3.2	0.58	0.68

For each CsEOF the best matching pattern (in terms of spatial correlation) is found. Due to slightly different time scales in the models the day at which the best match occurs may not correspond to that of the CsEOF. Note: data at all gridpoints are used in the calculation of the pattern correlation

After Sperber and Annamalai (2008).